Proceedings of the 12th International Conference on Fluid Flow, Heat and Mass Transfer (FFHMT 2025)
July 15, 2025 - July 17, 2025 | Imperial College London Conference, London, United Kingdom
Paper No. 221
DOI: 10.11159/ffhmt25.221

An End-to-End Methodology for CFD-based Parametric Optimisation of Propeller Boss Cap Fins

Divya Mehta[1], Om Inamdar[2], Gokul Rajaraman[2], Neeraj Kumbhakarna[2]
[1]Department of Aerospace Engineering, IIT Bombay
Mumbai, Maharashtra, 400076, India
[2]Department of Mechanical Engineering, IIT Bombay
Mumbai, Maharashtra, 400076, India
23b0001@iitb.ac.in; 23b2263@iitb.ac.in
22b4517@iitb.ac.in; neeraj_k@iitb.ac.in

Abstract – This research investigates the reduction in fuel consumption in the marine industry by reducing hub-vortex-related losses downstream of propellers using strategically placed fins. This study focuses on the parametric optimization of Propeller Boss Cap Fins (PBCFs) to establish the relationship between key design parameters and overall propeller efficiency. An ANSYS CFX-based CFD model was used to evaluate the impact of the various parameters on the overall efficiency. The variation in different parameters and their effects on efficiency are recorded and detailed in this paper. Furthermore, we present an end-to-end methodology that enables users to optimise their PBCF design for maximum efficiency. Our results show that the radius ratio has a dominant influence on efficiency due to eddy-induced losses, with the optimal configuration corresponding to the lowest feasible r/R, while phase angle variations have a marginal effect. This research contributes to the ongoing efforts to enhance marine propulsion efficiency, reduce fuel consumption, and mitigate environmental impact.

Keywords: Computational Fluid Dynamics, Turbulent Flow, Parametric Optimisation, Vortex dissipation, Ansys Automation, PBCF

1. Introduction

In light of environmental mandates, fossil fuel scarcity, and economic pressure, Energy Saving Devices (ESDs) have emerged as a topic of significant research interest. Propeller Boss Cap Fins (PBCFs) enhance propeller efficiency by disrupting the hub vortex and thereby increasing the thrust. Numerous studies [1-3] have evaluated the effects of PBCFs in open water conditions and considering hull interactions [4]. Currently, PBCFs are installed in over 2000 ships [3]. This study presents a methodology for optimizing Propeller Boss Cap Fins (PBCFs) to achieve maximum efficiency through design parameterization and a CFD-based analysis. The proposed approach is applied to the PPTC propeller, and general trends observed during the optimization process are discussed. The propeller efficiency is evaluated using the thrust (K_T), torque (K_Q), and advance coefficient (J) according to the following equations [1]:

$$K_T = \frac{T}{\rho n^2 D^4} \tag{1}$$

$$K_Q = \frac{Q}{\rho n^2 D^5} \tag{2}$$

$$J = \frac{V_A}{nD} \tag{3}$$

$$\eta = \frac{J K_T}{2\pi K_Q} \tag{4}$$

Where D is the propeller diameter, ρ denotes water density, V_A is the advance velocity and n denotes the rotations per second. T and Q denote the thrust and torque on the propeller respectively.

2. Method

In this section, we discuss the details of the geometric parameters that have been varied, as well as PPTC and PBCF mesh generation and boundary conditions. The open water simulation methodology, validated as in [2] is implemented. We further introduce a semi-automated simulation framework that significantly reduces the time required for each simulation, thereby enabling a higher number of simulations to be conducted within the same time frame. To model turbulent flow accurately, the SST (Shear Strength Transport) model with automatic wall functions was used, allowing adaptive near-wall treatment based on local mesh resolution for improved accuracy and efficiency.

2.1. Potsdam Propeller Test Case (PPTC)

For our CFD study, the Potsdam Propeller Test Case (PPTC) was chosen due to its status as a standard benchmark with extensive experimental data available for validation [2]. Table 1 presents the geometric parameters of the PPTC used for the simulations while Fig 1 depicts the structure of PPTC.

Table 1: Geometric Parameters of the PPTC

PPTC Parameters (with unit)	Notation	Value
Propeller Diameter (m)	D	0.255
Hub Diameter (m)	D_h	0.140
Number of blades	Z	5
Shaft Length (m)	L	0.365
Shaft Diameter (m)	D_S	0.0435

2.2. Propeller Boss Cap Fin (PBCF)

The PPTC and PBCF models were both designed in SolidWorks, where the PBCF was then assembled onto the PPTC to form the complete setup. Figs 2 and 3 depict the assembly of the PBCF on PPTC.

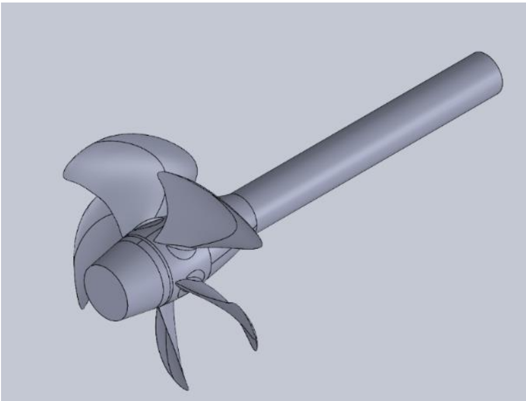

Fig 1: Isometric view of Potsdam Propeller Test Case

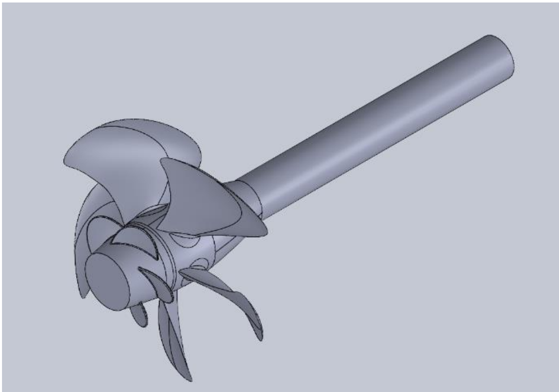

Fig 2: Isometric view of PBCF-assembly

The radius ratio (r/R) is defined as the ratio of the radius of the PBCF to the radius of the PPTC, while the phase angle (Φ) is the angle between the line passing vertically through the PPTC from the centre of the hub and the line passing through the nearest PBCF fin through the centre of the hub, as shown in Fig. 4.

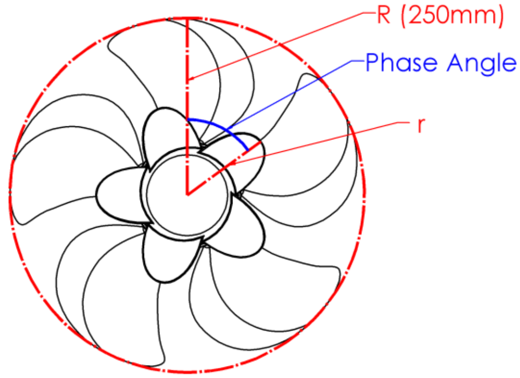

Fig 3: Illustration of PBCF parameters

In the initial phase of this study, only two parameters have been varied. Previous studies [5] have shown that the radius ratio is an important factor in determining overall efficiency; however, no documented research exists on the variation of the efficiency with respect to the phase angle. This motivated the choice to focus on these two parameters for the current analysis.

Additional parameters such as the thickness of the fins, the pitch angle of the helical fins of the PBCF, the distance between the PPTC and the PBCF, and the shape of the fins can be seamlessly integrated into the analysis using our automation methodology (discussed in section 2.4).

The PBCF has five fins and shows rotational symmetry every 72° in both directions. Therefore, it is sufficient to vary the phase angle between 0° and 72°. As the configurations at 0° and 72° are identical, the phase angle was varied from 0° to 63° in eight equal steps of 9°. The radius ratio was varied across 8 values, ranging from 0.26 to 0.50, with 0.26 representing the smallest physically possible value. This is because the radius ratio must be greater than the radius ratio of the hub and PPTC to allow the PBCF to extend outside the hub. The chosen intervals for both the phase angle and radius ratio are sufficiently small to cover all distinct cases necessary for assessing the effects of phase angle and radius ratio variations on efficiency. With 8 values for r/R and 8 for Φ, a total of 64 simulations were conducted to study the resulting trends.

2.3. Mesh and Boundary Conditions

A series of studies were performed to develop an optimal mesh (Fig 4 and 5) with regard to the computational time and accuracy of the solution. The automatic method was utilised, resulting in the generation of predominantly tetrahedral elements. Advanced meshing procedures such as inflation were used to generate hex-dominant structures on the layer of the blades along with a rotating mesh zone which was applied to the propeller and PBCF to ensure blade rotation at the required angular velocity. Key mesh metrics such as Element Quality, Aspect Ratio, Orthogonal Quality, and Skewness guided the iterative meshing process which has been encapsulated in Table 2.

Table 3: Average Mesh Metrics

	No. of Elements	Element Quality	Skewness	Orthogonal Quality	Aspect Ratio
Average	1134582	0.80	0.27	0.73	1.96

We used 10 layers of inflation and a growth rate of 1.2 which resulted in yplus values throughout the rotating domain remaining majorly under 300 as recommended by the SST model which further validates the accuracy of our model.

A mesh-independence study (Table 3) was conducted, where it was observed that the thrust and torque values showed negligible variation with further mesh refinement. As meshes 2 and 3 were each 10% finer than the preceding ones and showed only minor differences, mesh 1 was selected for the simulations to reduce computational time while maintaining accuracy.

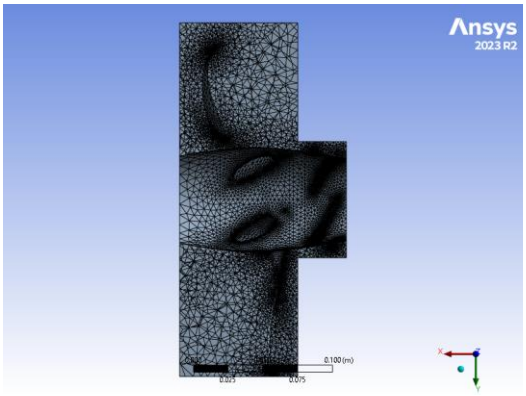

Fig 4: Mesh of Rotating Zone (PPTC+PBCF)

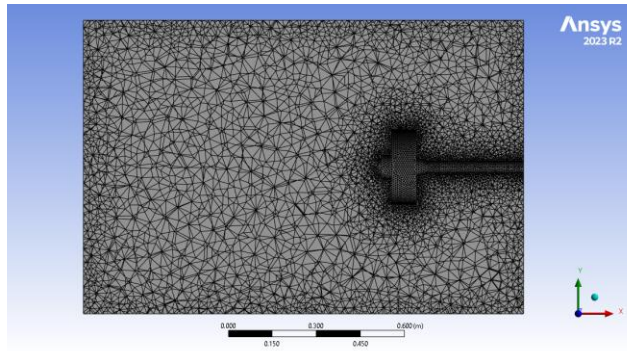

Fig 5: Mesh of non-rotating zone.

Table 3: Mesh Independence Study

	No. of Elements	J	Thrust (N)	K_T	Torque (N-m)	K_Q
Mesh 1	1082882	0.8	416.155	0.437	23.9662	0.098
Mesh 2	1214460	0.8	416.809	0.438	23.9441	0.098
Mesh 3	1378529	0.8	417.459	0.438	23.931	0.098

In all cases, the number of elements for the rotating domain are of the order 10^6 and that for the non-rotating domain are 10^5.

To model the water domain about the propeller, we have used a cylindrical water domain which is 4.3*D = 1.1 m downstream in length after the outlet. There is a shaft of length 0.365m connecting the propeller to the hull of the ship.

The setup and boundary conditions (Fig 4) for the open water simulations follow the methodology outlined in [1] and the results are validated with the same. A velocity profile was specified for the inlet boundary condition with J=0.8 and (1) and the rotating domain was assigned an angular speed of 15 revolutions/second in the positive x direction throughout while an atmospheric pressure field was applied at the outlet. The submerged propeller and shaft were assigned a no-slip (wall) condition. Interfaces were applied at the inlet, outlet, and shroud of the rotating and non-rotating domain. The threshold residuals for the simulations were set to 10^{-5} to maintain a balance between the computational time and accuracy of the simulation.

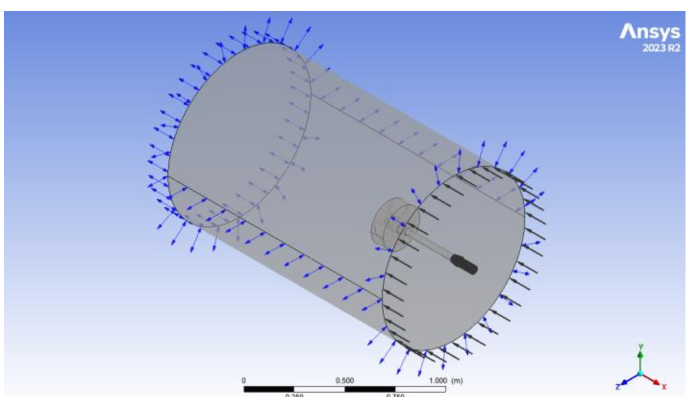

Fig 6: Boundary Conditions in CFX

2.4. Automation

Manual setup of simulations for parametric optimization is an extremely time-intensive process, as it involves importing each CAD model into ANSYS, configuring mesh connections, defining named selections and meshing parameters, linking to the CFX module, applying boundary conditions, and finally executing the solver. To address this, we developed a semi-automated workflow that significantly reduces the time and manual effort required for simulation setup and execution. A flowchart of this entire methodology is given in Fig 7 and the codes for the same can be obtained from [6]. This was performed in three different steps.

- A Python script was developed to externally control Ansys without using any GUI-based operations of Workbench. This code requires a folder of CADs as input and it creates a new single Ansys file that contains all the CADs connected to an Ansys mechanical module which is used for meshing and further connected to the CFX module for solving the simulation. This code reduces the time required to set up the Ansys Workbench for all the CADs by a factor of 3.
- Further automation was performed on the meshing where we created a script for meshing via scripting offered by Ansys Mechanical. This code created the face sizing, meshing method and inflation feature. It also creates all the named selections as Ansys generates the face IDs for fluid domains and all CADs present in the same Workbench file in the same manner. This reduced the time required per simulation by a factor of 10.
- The final part of our automation was to set up the CFX boundary conditions. This was done through a '.ccl' script which can be imported into CFX-pre directly. The script consists of all the boundary conditions, data required for setting up the rotating and non-rotating domains and the solver control settings. This process reduced the time required to model the boundary conditions per simulation by a factor of 15.

This partially automated method reduced the time to model each simulation by a factor of 11 (~35 minutes saved). Other than saving time, it mitigates any possibility of human error while modelling a large number of simulations manually while making sure all the simulations have exactly identical conditions.

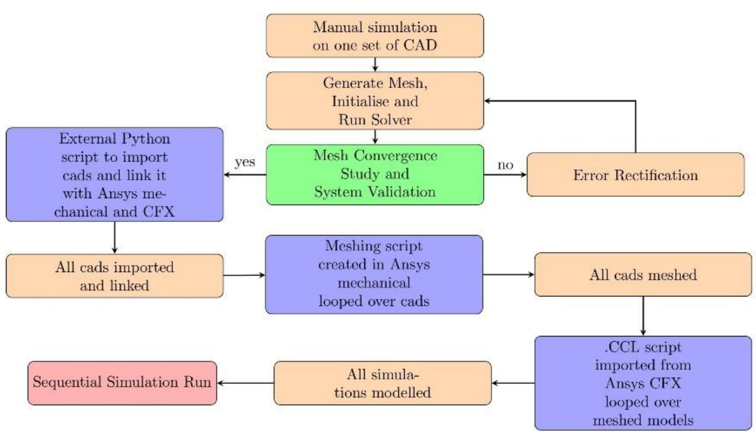

Fig 7: Flowchart describing overall automation methodology

3. Results and Discussion

The simulations in all the cases have been performed at a constant angular speed of 15 revolutions per second and a constant inlet velocity corresponding to J=0.8. All of the simulations have been performed using a computer with the following specifications: Intel® i5 12th gen CPU and 16 usable cores.

The results tabulated in Table 4 indicate a ~10-15 % increase in the efficiency following the installation of PBCF. Table 4 includes data for PPTC, the best configuration and the worst configuration indicating that all the configurations that have been run have higher efficiencies than PPTC.

Table 4: Increase in efficiency post-PBCF installation

Configuration	K_T	K_Q	η
PPTC	0.33688	0.0998	0.4294
Best PBCF configuration	0.459	0.100	0.5836
Worst PBCF configuration	0.386	0.0952	0.5175

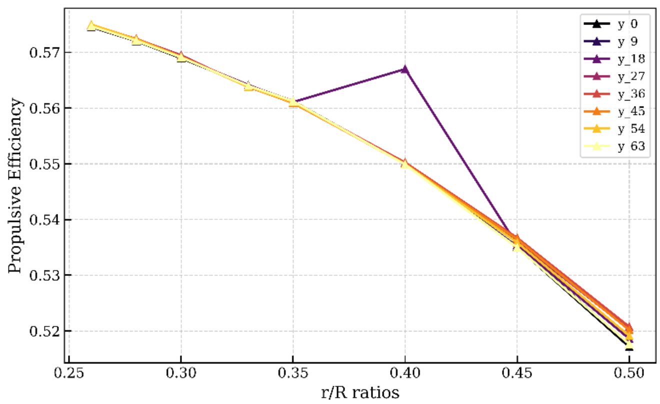

Fig 8: Efficiency v/s r/R at various Phase Angles

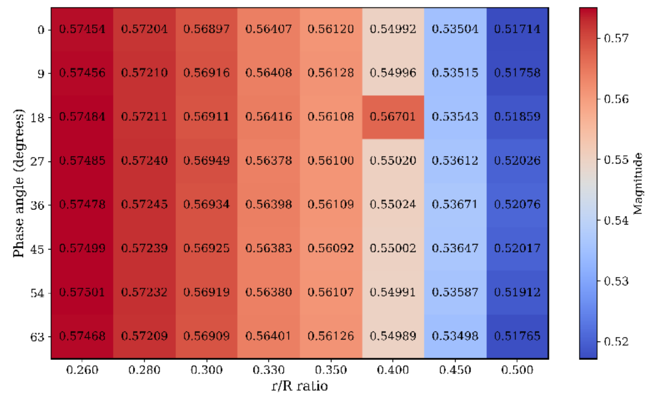

Fig 9: Efficiency Heatmap: Phase Angle vs r/R

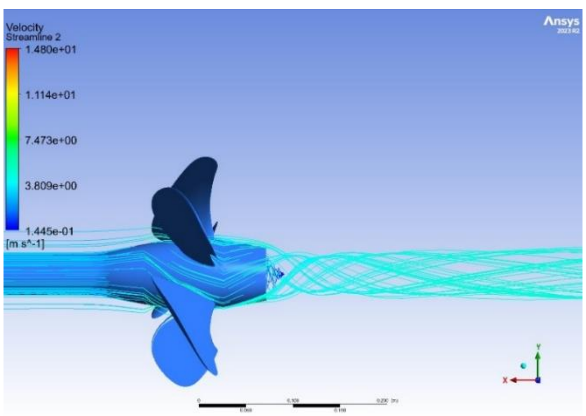

Fig 10: PPTC Streamlines

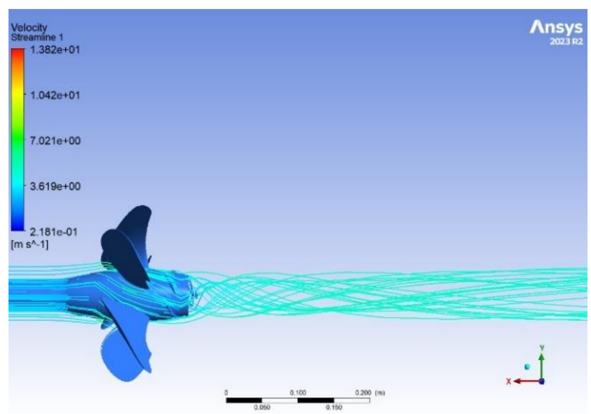

Fig 11: PBCF Streamlines (r/R=0.26, Φ= 27)

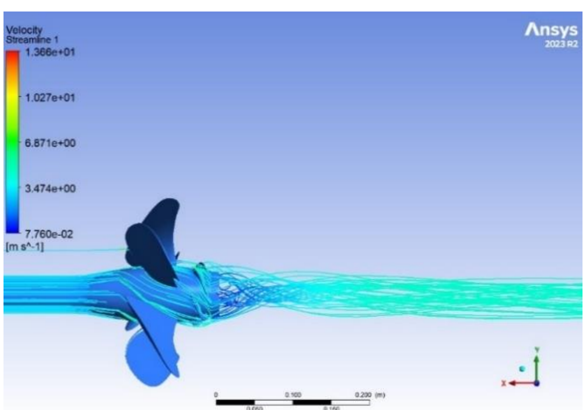

Fig 12: PBCF Streamline (r/R=0.33, Φ= 27)

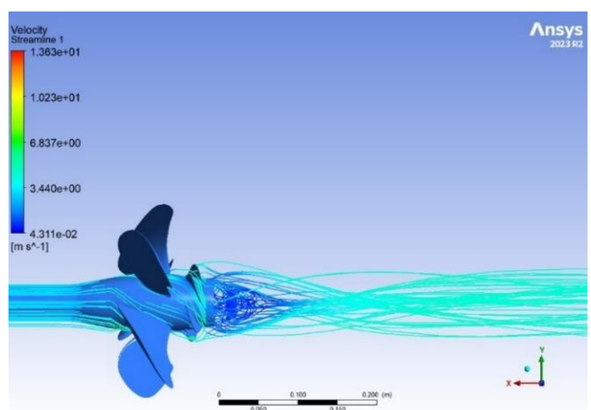

Fig 13: PBCF Streamlines (r/R=0.40, Φ= 27)

Fig 8 represents the variation of efficiency with r/R at various phase angles. We observe that the efficiency decreases with an increase in r/R and changes only marginally with phase angle change. Fig 9 is a heatmap which helps us visualise the results. Fig 10 represents the streamlines for PPTC while Fig 11-13 represent the streamlines for configurations of PBCF at the same phase angle and different r/R. As observed in Fig 17, there is a region of low pressure created [7] at the centre of the hub at the outlet, and since the flow is in the direction from low to high pressure, there is an adverse pressure gradient created. This adverse pressure gradient causes the streamline to flow back, leading to the formation of eddies [8]. We can observe the mitigation of hub vortex in all configurations of PBCF as compared to the PPTC which increases the efficiency of the propeller. Eddy viscous effects are higher in PPTC (Fig 14) than at lower r/R(0.26-0.33) (Fig 16), with greater hub vortex mitigation at higher r/R (Fig 18). However, increased eddy viscous losses at higher r/R reduce overall propeller efficiency compared to lower r/R.

These eddies lead to energy losses in the flow via turbulent viscous effects. The size of the low-pressure region after the hub at higher values of r/R is observed to be greater (Fig 19) which leads to more eddy losses (Fig 18) and overall a lower propeller efficiency.

Variation of efficiency with phase angle is marginally small as it changes after the 4th decimal. Variation at higher r/R is much higher as compared to lower r/R, this can be explained through the better mesh statistics at lower r/R hence higher r/R meshes have more numerical errors explaining the trend. All the data for the simulations [5] is also available.

The simulation at r/R=0.40 and Φ=9 is an outlier in our set of simulations as seen in Fig 8. This is likely due to interpolation errors [9] at mesh interfaces, which can introduce local numerical inaccuracies, especially in regions with non-conformal grids or steep gradients.

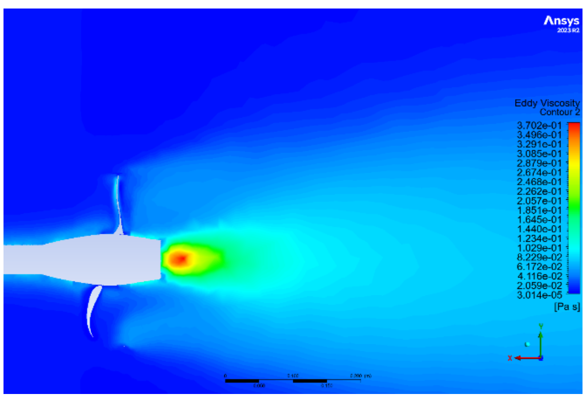

Fig 14: Eddy Viscosity Contour for PPTC

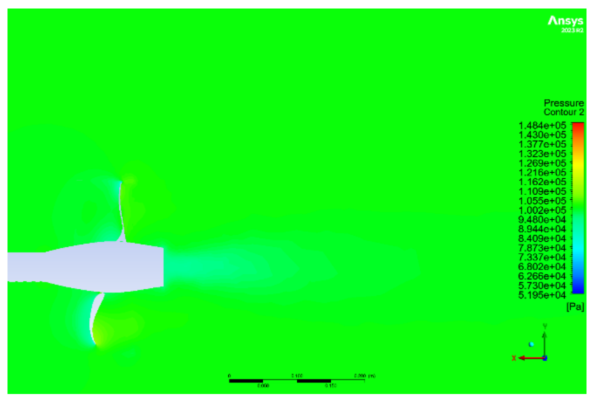

Fig 15: Pressure Contour for PPTC

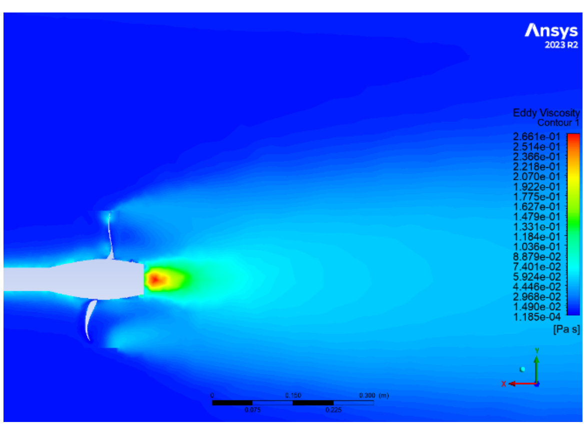

Fig 16: Eddy Viscosity Contour for r/R=0.26, Φ= 27

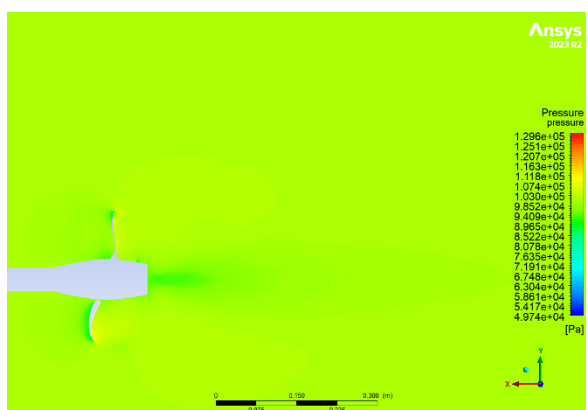

Fig 17: Pressure Contour for r/R=0.26, Φ= 27

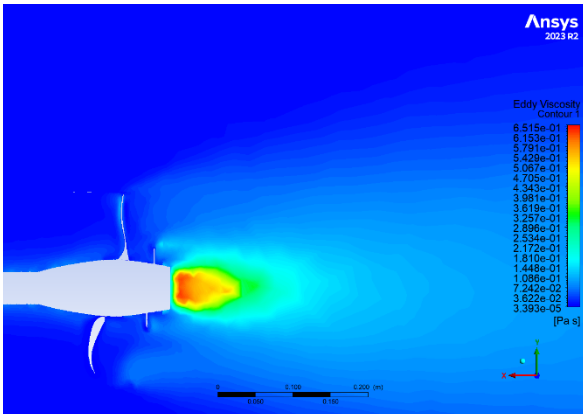

Fig 18: Eddy Viscosity Contour for r/R=0.50, Φ= 27

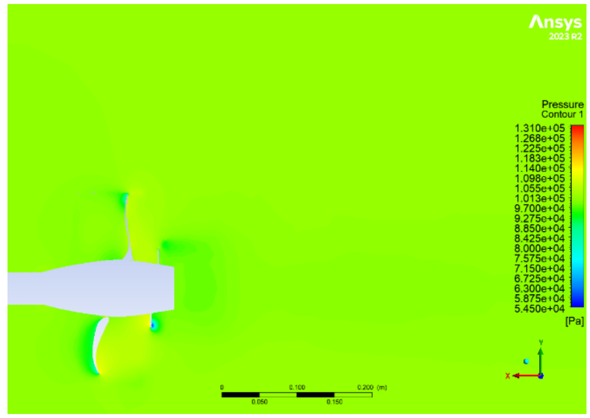

Fig 19: Pressure Contour for r/R=0.50, Φ= 27

4. Conclusion

This study explored the impact of various geometric parameters on the efficiency of PBCFs. The radius ratio had a significant impact on the efficiency, varying from ~52%-57% as the r/R decreases which was explained by the eddy viscous effects formed due to the adverse pressure gradient. The most optimal radius ratio of the PBCF for the PPTC chosen is the geometrically least possible r/R, keeping the width of the fin constant. The phase angle had a very marginal effect. This study does not account for cavitation effects, which could result in additional losses.

The scope for future studies developing a Python package for complete automation wherein the most optimised configuration can be found out via CFD simulations by just having a single PBCF assembly CAD as an input, varying various other parameters which can be integrated into this research via our automation methodology and also studying cavitation and hull effects.

With over 2000 ships currently equipped with PBCFs, the practical benefits of these devices are evident. This research contributes to the ongoing efforts to enhance marine propulsion efficiency, reduce fuel consumption, and mitigate environmental impact.

References

[1] K. Mizzi, Y. K. Demirel, C. Banks, O. Turan, P. Kaklis, and M. Atlar, "Design optimisation of Propeller Boss Cap Fins for enhanced propeller performance," *Appl. Ocean Res.*, vol. 62, pp. 210–222, 2017

[2] A. Verma, M. Kapoor, and N. Kumbhakarna, "Investigation of hydrodynamic performance in marine propellers with modified blade design," in *Proc. 10th Int. Conf. on Fluid Flow, Heat and Mass Transfer (FFHMT'23)*, 2023

[3] T. Kawamura, K. Ouchi, and T. Nojiri, "Performance analysis of energy saving devices with model tests and numerical simulation," *J. Mar. Sci. Technol.*, vol. 17, pp. 1–12, 2012

[4] G.Rajaraman. P.Tomar and N.Kumbhakarna, "Design and Parametric Analysis of Propeller Boss Cap Fins with Hull Interaction Effects: A CFD-based Study" in *Proc. International Conference of Flow Dynamics, 2024*

[5] S.-S. Lim, T.-W. Kim, D.-M. Lee, C.-G. Kang, and S.-Y. Kim, "Parametric study of propeller boss cap fins for container ships," *Int. J. Nav. Archit. Ocean Eng.*, vol. 6, no. 2, pp. 187–205, 2014

[6] OmDivya-Research, "FFHMT-2025: Parametric Optimization of PBCFs," GitHub, 2025. [Online]. Available: https://github.com/OmDivya-Research/FFHMT-2025/tree/main

[7] I. Funeno, "On viscous flow around marine propellers —Hub vortex and scale effect—," *Journal of the Kansai Society of Naval Architects, Japan*, vol. 2002, no. 238, pp. 17–27, 2002.

[8] J. D. Anderson, *Fundamentals of Aerodynamics*, 3rd ed. Boston, MA: McGraw-Hill, 2001, p. 280.

[9] NASA Glenn Research Center, "Uncertainity and Error in CFD Simulations," *NASA*, Jun. 9, 2004. [Online]. Available: https://www.grc.nasa.gov/WWW/wind/valid/tutorial/errors.html